

Brain charts for the human lifespan

Bethlehem, R.A.I.^{1,2,#}, Seidlitz J.^{3,4,#}, White, S.R.^{5,6,#}, Vogel, J.W.^{7,3}, Anderson, K.M.⁸, Adamson C.^{9,10}, Adler, S.¹¹, Alexopoulos, G.S.¹², Anagnostou, E.^{13,14}, Areces-Gonzalez, A.¹⁵, Astle, D.E.¹⁶, Auyeung B.^{17,1}, Ayub, M.¹⁸, Ball G.^{9,19}, Baron-Cohen, S.^{1,20}, Beare, R.^{9,10}, Bedford, S.A.¹, Benegal V.²¹, Beyer, F.²², Bin Bae, J.²³, Blangero, J.²⁴, Blesa Cábez, M.²⁵, Boardman, J.P.²⁵, Borzage, M.²⁶, Bosch-Bayard, J.F.^{27,28}, Bourke, N.²⁹, Calhoun, V.D.³⁰, Chakravarty, M.M.^{31,28}, Chen, C.³², Chertavian, C.³, Chetelat, G.³³, Chong, Y.S.^{34,35}, Cole, J.H.^{36,37}, Corvin, A.³⁸, Courchesne, E.^{39,40}, Crivello, F.⁴¹, Croypley, V.L.⁴², Crosbie, J.⁴³, Crossley, N.^{44,45}, Delarue, M.⁴⁶, Desrivieres, S.⁴⁷, Devenyi, G.^{48,49}, Di Biase, M.A.^{42,50}, Dolan, R.^{51,52}, Donald, K.A.⁵³, Donohoe G.⁵⁴, Dunlop, K.⁵⁵, Edwards, A.D.^{56,57}, Elison, J.T.⁵⁸, Ellis, C.T.⁸, Elman, J.A.⁵⁹, Eyer L.^{60,61}, Fair, D.A.⁵⁸, Fletcher, P.C.^{62,63}, Fonagy, P.⁶⁴, Franz, C.E.⁶⁵, Galan-Garcia, L.⁶⁶, Gholipour, A.⁶⁷, Giedd, J.⁶⁸, Gilmore, J.H.⁶⁹, Glahn, D.C.^{70,71}, Goodyer, I.⁵, Grant, P.E.⁷², Groenewold, N.A.^{73,74}, Gunning, F.M.¹², Gur, R.E.^{3,75}, Gur, R.C.^{3,76}, Hammill, C.F.^{43,77}, Hansson, O.^{78,79}, Hedden T.^{80,81}, Heinz A.⁸², Henson R.^{16,83}, Heuer K.^{84,85}, Hoare J.⁸⁶, Holla B.⁸⁷, Holmes, A.J.⁸⁸, Holt R.¹, Huang H.^{89,90}, Im, K.^{91,92}, Ipser, J.⁹³, Jack Jr, C.R.⁹⁴, Jackowski, A.P.^{95,96}, Jia, T.^{97,98,99}, Johnson, K.A.^{100,101,71}, Jones, P.B.^{5,103}, Jones, D.T.^{104,105}, Kahn, R.^{106,107}, Karlsson H.^{108,109,110}, Karlsson L.^{108,109,110}, Kawashima R.¹¹¹, Kelley, E.A.¹¹², Kern S.¹¹³, Kim, K.^{114,115,116}, Kitzbichler, M.G.⁵, Kremen, W.S.⁵⁹, Lalonde, F.¹¹⁷, Landeau, B.³³, Lee, S.¹¹⁸, Lerch, J.^{119,120,121}, Lewis, J.D.¹²², Li, J.¹²³, Liao W.¹²³, Linares, D.P.¹⁵, Liston, C.¹²⁴, Lombardo, M.V.^{125,1}, Lv, J.^{42,126}, Lynch, C.⁵⁵, Mallard, T.T.¹²⁷, Marcelis, M.¹²⁸, Markello, R.D.¹²⁹, Mazoyer, B.^{41,130}, McGuire, P.¹³¹, Meaney, M.J.¹³², Mechelli, A.¹³¹, Medic, N.⁵, Mistic, B.¹²⁹, Morgan, S.E.^{133,134,135}, Mothersill D.^{136,137,138}, Nigg J.¹³⁹, Ong, M.Q.W.¹⁴⁰, Ortinau C.¹⁴¹, Ossenkoppele, R.^{142,143}, Ouyang, M.⁸⁹, Palaniyappan, L.¹⁴⁴, Paly, L.¹⁴⁵, Pan, P.M.^{146,147}, Pantelis, C.^{148,149,150}, Park, M.M.¹⁵¹, Paus, T.^{152,153}, Pausova, Z.^{43,154}, Pichet Binette, A.^{155,156}, Pierce, K.¹⁵⁷, Qian, X.¹⁴⁰, Qiu, J.¹⁵⁸, Qiu, A.¹⁵⁹, Raznahan, A.¹¹⁷, Rittman, T.¹⁶⁰, Rollins, C.K.^{161,162}, Romero-Garcia, R.⁵, Ronan, L.⁵, Rosenberg, M.D.¹⁶³, Rowitch, D.H.¹⁶⁴, Salum, G.A.^{165,166}, Satterthwaite, T.D.^{7,3}, Schaare, H.L.^{167,168}, Schachar, R.J.⁴³, Schultz, A.P.^{100,169,71}, Schumann, G.^{170,171,172}, Schöll, M.^{173,174,175}, Sharp, D.²⁹, Shinohara, R.T.^{32,176}, Skoog, I.¹¹³, Smyser, C.D.¹⁷⁷, Sperling, R.A.^{100,101,71}, Stein, D.J.¹⁷⁸, Stolicyn, A.¹⁷⁹, Suckling J.⁵, Sullivan, G.²⁵, Taki, Y.¹¹¹, Thyreau B.¹¹¹, Toro, R.^{180,85}, Tsvetanov, K.A.^{160,181}, Turk-Browne, N.B.^{8,182}, Tuulari, J.J.^{183,184,185}, Tzourio, C.¹⁸⁶, Vachon-Preseu, É.^{187,188,189}, Valdes-Sosa, M.J.⁶⁶, Valdes-Sosa, P.A.^{15,190}, Valk, S.L.¹⁹¹, van Amelsvoort, T.¹⁹², Vandekar, S.N.^{193,194}, Vasung, L.¹⁹⁵, Victoria, L.W.¹², Villeneuve, S.^{156,196,155}, Villringer, A.^{22,197}, Vértes, P.E.^{5,198}, Wagstyl, K.¹⁹⁹, Wang, Y.S.^{200,201,202}, Warfield, S.K.⁶⁷, Warrior, V.¹, Westman, E.²⁰⁴, Westwater, M.L.⁵, Whalley, H.C.¹⁷⁹, Witte, A.V.^{197,22,205}, Yang, N.^{200,201,206}, Yeo, B.T.T.^{207,208,209}, Yun, H.J.²¹¹, Zalesky, A.²¹², Zar, H.J.^{73,213}, Zettergren, A.¹¹³, Zhou, J.H.^{140,214,207}, Ziauddeen, H.^{5,215,216}, Zugman, A.^{217,218}, Zuo, X.N.^{200,201,206}, AIBL*, Alzheimer's Disease Neuroimaging Initiative**, Alzheimer's Disease Repository Without Borders Investigators***, CALM Team****, Cam-CAN*****, CCNP, 3R-BRAIN*****, COBRE*****, ENIGMA Developmental Brain Age working group*****, Harvard Aging Brain Study*****, IMAGEN, KNE96*****, NSPN*****, POND*****, The PREVENT-AD Research Group, VETSA, Bullmore, E.T.⁵, Alexander-Bloch, A.F.^{3,4}

equal contribution

Abstract

Over the past 25 years, neuroimaging has become a ubiquitous tool in basic research and clinical studies of the human brain. However, there are no reference standards against which to anchor measures of individual differences in brain morphology, in contrast to growth charts for traits such as height and weight. Here, we built an interactive online resource (www.brainchart.io) to quantify individual differences in brain structure from any current or future magnetic resonance imaging (MRI) study, against models of expected age-related trends. With the goal of basing these on the largest and most inclusive dataset, we aggregated MRI data spanning 115 days post-conception through 100 postnatal years, totaling 122,123 scans from 100,071 individuals in over 100 studies across 6 continents. When quantified as centile scores relative to the reference models, individual differences show high validity with non-MRI brain growth estimates and high stability across longitudinal assessment. Centile scores helped identify previously unreported brain developmental milestones and demonstrated increased genetic heritability compared to non-centiled MRI phenotypes. Crucially for the study of brain disorders, centile scores provide a standardised and interpretable measure of deviation that reveals new patterns of neuroanatomical differences across neurological and psychiatric disorders emerging during development and ageing. In sum, brain charts for the human lifespan are an essential first step towards robust, standardised quantification of individual variation and for characterizing deviation from age-related trends. Our global collaborative study provides such an anchorpoint for basic neuroimaging research and will facilitate implementation of research-based standards in clinical studies.

Main

First published in the late 18th century ¹, the simple framework of growth charts to quantify developmental change against a reference standard remains a cornerstone of paediatric care. Although a powerful example of “personalised” or “precision” medicine, growth charts exist mainly for a small set of anthropometric variables (e.g., height, weight and head circumference). Critically, brain growth and maturation continues well beyond the developmental periods covered by anthropometric charts. The lack of brain reference standards is particularly relevant to psychiatric disorders that are increasingly considered to be disorders of neurodevelopment² and arguably represent the single highest current global health burden ³. Furthermore, preterm infants and those born with congenital conditions – many with psychiatric sequelae – show marked morphological differences during early brain development ^{4–7} and even decades later during adulthood ^{7,8}. With ageing, neurodegeneration and accelerated overall reductions in brain tissue volume are hallmark signatures of Alzheimer’s disease ⁹ and other types of dementia. Modernising the concept of growth charts to generate analogous life-spanning reference charts for the human brain would allow for standardised comparison across samples at scale, while simultaneously advancing our understanding of atypicality by providing benchmark reference points for both typical development and ageing.

Standards for neuroimaging-based reference charts have not yet materialised, likely due to challenges of integration across studies targeting specific but often disjointed developmental epochs and clinical conditions. In particular, the period from fetal growth through early postnatal development (<4-6 years) is rarely incorporated, despite evidence that early molecular and mechanical processes shape growth trajectories ^{10,11} and vulnerability to psychiatric conditions ¹². Case-control comparisons are usually limited to a single disorder, despite evidence of shared risk factors and mechanisms in psychiatric disorders ^{13,14}. Additionally, compared to anthropometric growth charts, neuroimaging is more sensitive to technological variation in scanner platforms, acquisition, and analytic strategy. Collaborative initiatives spurring collection of large-scale datasets ^{15–17}, recent advances in imaging-processing ¹⁸, and proven statistical frameworks ^{19,20} provide the building blocks for comprehensive life-spanning reference charts of the human brain. Here, we present lifespan models of brain development and ageing that i) robustly capture the normative spectrum of age and sex; ii) identify previously unreported brain growth milestones; iii) increase sensitivity to genetic and early life events; iv) provide standardised effect-size deviations that reveal new patterns of neuroanatomical differences across multiple clinical disorders; and v) represent a global resource for future neuroimaging studies to leverage the benefits of reference-based measures.

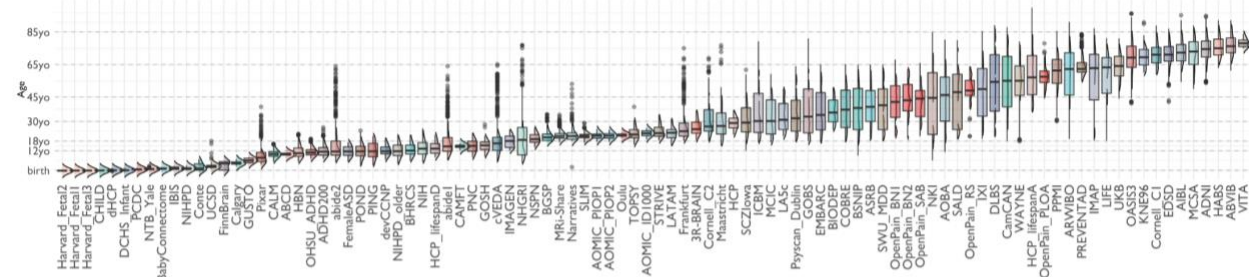
Mapping normative brain growth

We created brain charts for the human lifespan using generalised additive models for location, scale and shape (GAMLSS) ^{19,20}, a robust and flexible framework for modelling non-linear growth trajectories recommended by the World Health Organization ²⁰. Models were based on cross-sectional healthy volunteer data of the major cerebral brain tissue classes derived from structural magnetic resonance imaging (MRI): total cortical grey and white matter, total subcortical grey matter and total ventricular volume (see Methods and Supplementary Information [SI1]). Our sex-

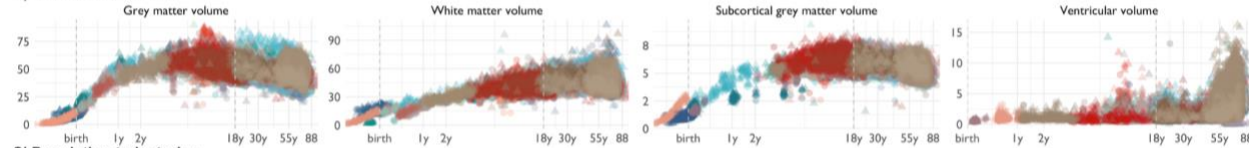
stratified models incorporated variation in site and processing pipeline to allow computation of standardised reference charts. The brain tissue classes from 96 studies (Fig. 1A, SI Table 1, SI Data Descriptions) showed clear, predominantly age-related trends, even prior to any modelling (Fig. 1B). Yet, marked heterogeneity of growth curves for individual studies (SI2) reinforces the importance of using the full aggregated dataset to achieve representative norms not biased by individual studies. The validity of the models is supported by high stability under cross-validation and bootstrap resampling (SI2). Comparing these models to multiple non-MRI metrics of brain size demonstrated high correspondence across the lifespan (SI2).

Our models extend previously reported growth curves in multiple ways. Lifespan curves (Fig 1C) show an initial strong increase in total cortical grey matter volume (GMV) from mid-gestation onwards, peaking at 6.3 years postnatal (bootstrapped confidence intervals = CI_{Boot} : 6-6.4 years), followed by a near linear decrease. The observed peak occurs 2-3 years later than prior reports relying on smaller age-restricted samples^{21,22}. Cerebral white matter volume (WMV) also increased rapidly from mid-gestation through early childhood, when rate-of-growth slowed before peaking at 28.9 years postnatal (CI_{Boot} : 28.4-29.5 years), with subsequent accelerated decline in WMV after 50. Subcortical grey matter volume (sGMV) showed an intermediate growth pattern to GMV and WMV, with rate-of-growth peaking in adolescence at 14.7 years (CI_{Boot} : 14.3-15.1 years). Both the WMV and sGMV peaks are consistent with prior neuroimaging and postmortem reports^{23,24}. In contrast, ventricular cerebrospinal fluid volume (CSF) showed an increase until age 2, followed by a plateau until age 30 and a slow linear increase that exponentiated in the sixth decade of life. Total cerebrum volume (TCV), an aggregate of the above features, showed the highest rate of increase in infancy, peaking in adolescence at 13.3 years, and declining steadily until age 55 when the decline accelerated (SI3). Previously reported growth curve models have not, in general, modelled age-related changes in the variability of brain structure. Age-related variance (Fig. 1D), explicitly estimated by GAMLSS, formally demonstrates developmental changes in across-individual variability. There was an early developmental increase in GMV and sGMV variability that peaked at 5 years and subsequently declined. In contrast, WMV variability peaked during the fourth decade of life, and CSF was maximally variable at the end of the human lifespan (Fig. 1D). In line with prior literature²⁵, variance in males is higher than in females across imaging phenotypes. These variance differences across development demonstrate the importance of modelling age and sex-related differences in variability in addition to absolute size.

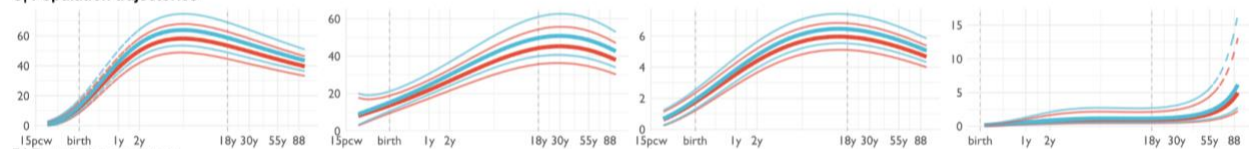
A) Aggregated MRI Datasets



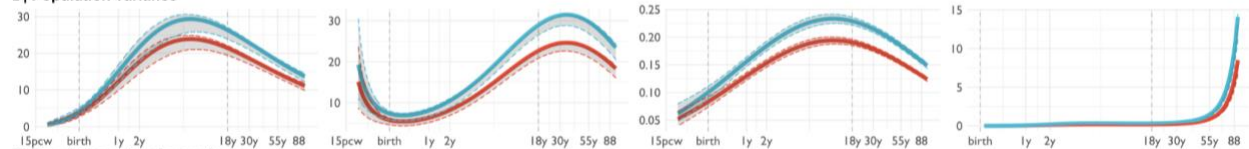
B) Total tissue volume



C) Population trajectories



D) Population variance



E) Population rate-of-growth

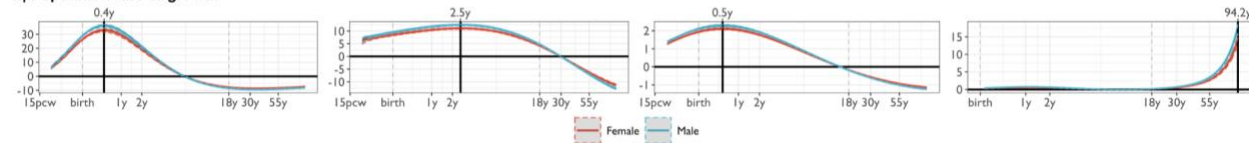


Fig. 1: Neuroimaging growth charts. A) MRI data were aggregated from 96 primary studies of 120,685 scans collectively spanning the age range from late pregnancy to 100 postnatal years. Box-violin plots show age distributions (log-scaled) of each study. B) Raw, non-centiled bilateral volume estimates plotted for each participant, coloured by study, as a function of age (log-scaled) and scaled to $10,000\text{mm}^3$. C) Normative growth curves estimated by generalised additive modelling for location scale and shape (GAMLSS), accounting for study offsets, processing pipeline, stratified by sex (female/male as red/blue) and providing reference centile boundaries of 95% (dotted lines), analogous to a paediatric growth chart. D) Across-individual variance with the 95% confidence interval determined by 1000 bootstraps stratified by sex. E) Rate of change across the lifespan (first derivative of the primary trajectory) stratified by sex, with solid black lines at zero (where the sign of the trajectory flips) and at age of peak growth (exact year denoted on the top mirrored x-axis).

Developmental milestones

Neuroimaging milestones are defined by inflection points of the tissue-specific volumetric trajectories (Fig. 2, Methods). Relative to traditional pubertal age milestones²⁶, only GMV peaked before typical pubertal onset, with sGMV peaking mid-puberty and WMV peaking in young adulthood (Fig. 2). The rate-of-growth (velocity) peaked for GMV (5.08 months, CI_{Boot} : 4.85-5.22 months), sGMV (5.65 months, CI_{Boot} : 5.75-5.83) and WMV (2.5 years, CI_{Boot} : 2.4-2.6 years) in infancy and early childhood. TCV velocity peaked between the maximum velocity for GMV and WMV at ~7 months. Two major milestones of TCV and sGMV (peak velocity and peak size; Fig. 2) coincided with the early neonatal and adolescent peaks of height and weight velocity^{27,28}.

These velocity peaks in early infancy have not been reported previously due to the lack of incorporation of prenatal datasets to allow for the modelling of rapid early growth^{23,29}.

It has been hypothesized that age-varying cellular processes could be captured by these neuroimaging milestones, in terms of the relative growth trajectories of macroscopic volumetric measurements³⁰. In our dataset, we find an initial postnatal increase in GMV relative to WMV, likely due to increased complexity of neuropil including synaptic proliferation^{31,32}. Subsequently, GMV declines relative to WMV, likely due to both continued myelination and synaptic pruning³³. The exact timing of the GMV:WMV differentiation in early development has not been clearly demarcated by prior studies, partly due to the lack of data spanning the prenatal period. In contrast, lifespan growth curves demarcate an early period of GMV:WMV differentiation, beginning with the switch from WMV to GMV as the majority tissue compartment in the first month after birth (GMV/WMV ratio = 1), and ending when the absolute difference of GMV and WMV peaked around 3.5 postnatal years. This epoch of GMV:WMV differentiation overlaps with the period of greatest change in brain metabolites³⁴ (0-3 postnatal months) and the brain's resting metabolic rate (RMR; minimum=7 months, maximum=4.2 years)³⁵, as well as the typical period of acquisition of motor capabilities³⁶ (Fig. 2).

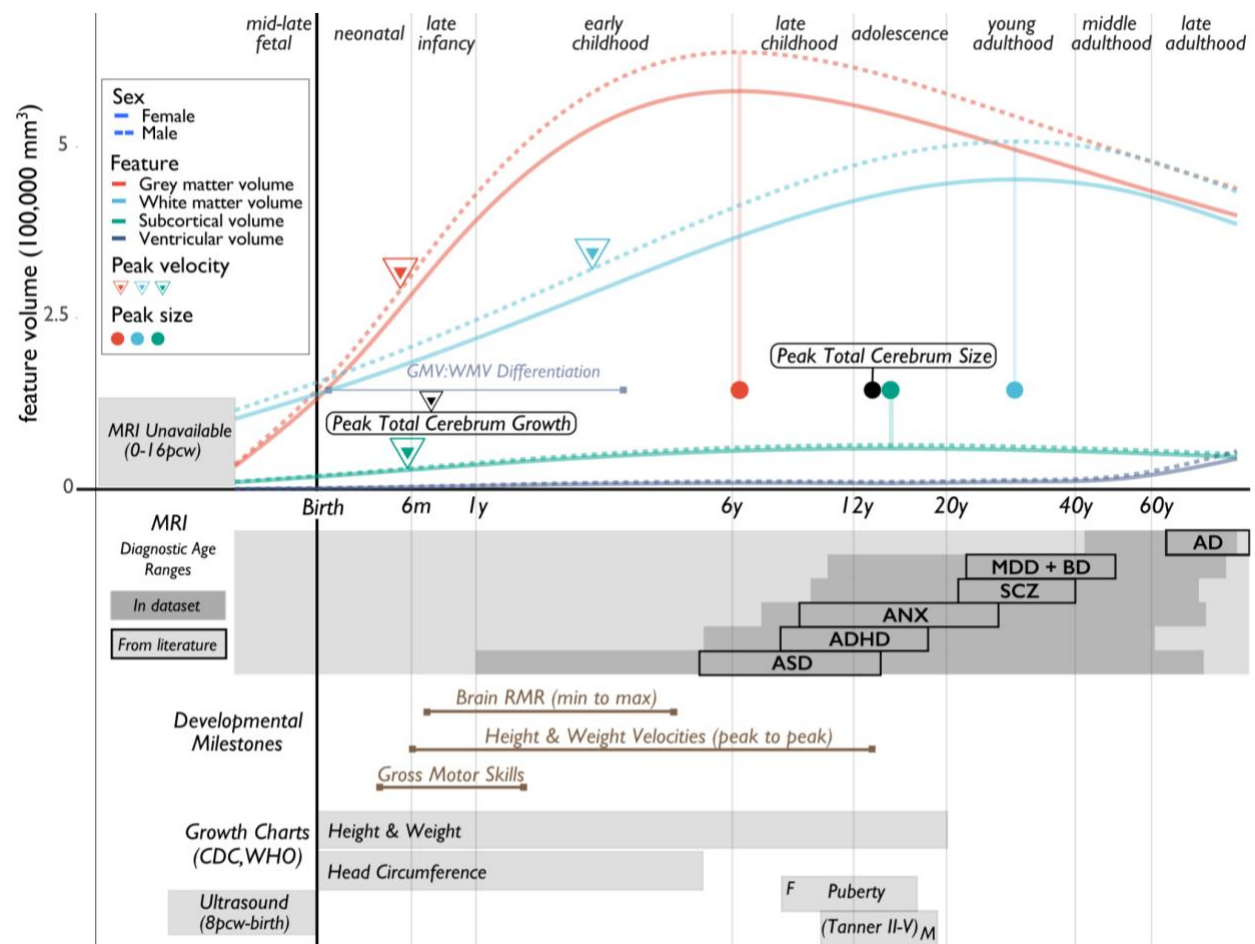


Fig. 2: Neurodevelopmental milestones, Summary of the reference norms (50th centile) for each tissue class and derived milestones as a function of age (log-scaled). Circles depict peak absolute values for each tissue type (point where velocity crosses zero in Fig. 1E), whereas triangles depict peak velocity (peaks in Fig. 1E). Top grey sections

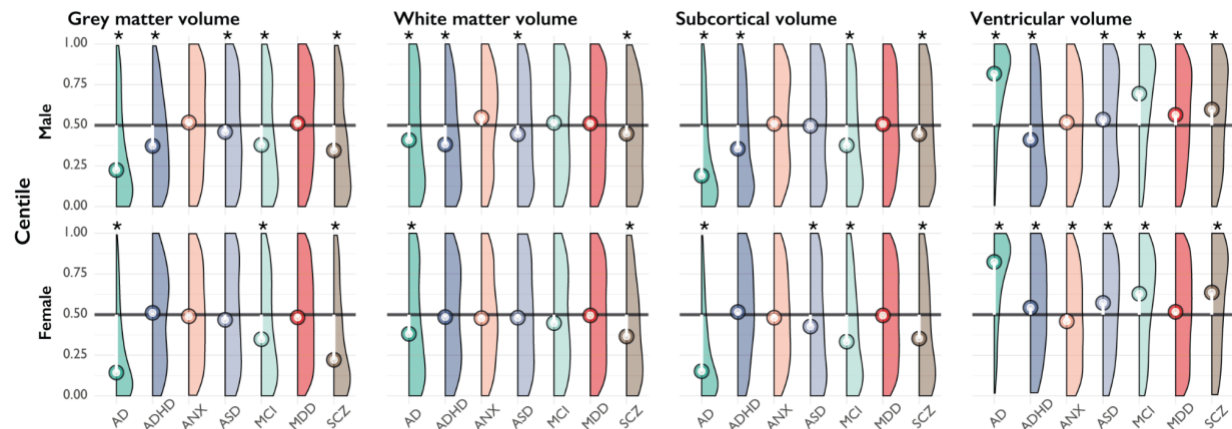
denote the age-range of the current lifespan neuroimaging (MRI) study, with empirical age-ranges (dark grey) for a subset of clinical conditions plotted against diagnostic age ranges derived from the literature (black outlines; Methods). Bottom grey sections depict overall age ranges for typical anthropometry and ultrasonography. Non-MRI developmental milestones are approximated based on previous literature and averaged across males and females (see Methods). Light grey vertical lines define lifespan epochs adapted from previous molecular neurobiological boundaries³⁷. Abbreviations; resting metabolic rate (RMR), Alzheimer's Disease (AD), Attention Deficit Hyperactivity Disorder (ADHD), Anxiety or Phobia (ANX), Autism Spectrum Disorder (ASD) including high-risk individuals with confirmed diagnosis at a later age, Major Depressive Disorder (MDD), Bipolar Disorder (BD), Schizophrenia (SCZ).

Individualised centiles in clinical samples

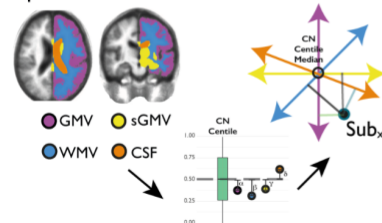
We computed harmonised, individualised centile scores that leverage information about expected age-related trends from the reference charts (SI Methods). Moreover, the clinical diversity of the aggregated dataset allowed us to comprehensively investigate case-control differences in individually-specific centile scores. Relative to the control group (CN), there were highly significant differences in centiles across large ($n > 500$) diagnostic groups (Fig. 3A; SI tables 2 and 3). The pattern of these centile differences varied across tissue types and disorders (Fig. 3A, SI7). In addition, we generated a cumulative deviation metric, the “centile Mahalanobis distance” (CMD), across all brain phenotypes relative to the CN median, to summarise a comparative assessment of brain morphology (Fig 3B, Methods, SI1.6). Alzheimer's disease (AD) showed the greatest overall difference across disorders sampled, with a maximum difference localized to gray matter in biologically female patients (difference from CN median = 36%; Fig. 3A-B, SI7). Notably, schizophrenia ranked third overall behind AD and mild cognitive impairment (MCI), based on CMD (Fig. 3C, SI7). Although different mechanisms underlie the neuroanatomical abnormalities observed in AD and schizophrenia³⁸, and in the case of schizophrenia the cellular basis remains to be fully elucidated, cortical grey matter loss has been associated with cognitive impairment and psychiatric symptomatology in both disorders³⁹. Assessment across diagnostic groups, based on patterns of the multiple centile scores and CMD, highlighted the relative specificity of brain profiles across clinical conditions (SI8). However, when examining cross-disorder similarity, hierarchical clustering yielded three clusters broadly comprising neurodegenerative, mood/anxiety, and neurodevelopmental disorders (SI8). Overall, these analyses highlight the complementary use-cases for examining both the absolute and relative differences in centiles within and across conventional diagnostic categories.

Interindividual variation in centile scores and deviation also showed strong associations with development, early-life events, and shared genetic architecture. Across individual lifespan epochs, CMD was consistently greater in patients relative to controls irrespective of diagnostic category, with the largest difference found in adolescence (3.3-7.4% across epochs³⁷; SI4). Adolescence also represents the greatest period of overlap across diagnostic categories in our dataset and a period of overall vulnerability for neuropsychiatric disease onset (Fig. 2). In 5 independent samples across the lifespan, average centile scores were related to multiple metrics of premature birth (gestational age at birth: $t=13.164$, $P<2e-16$; birth weight: $t=36.395$, $P<2e-16$; SI5). Centile scores also showed increased twin-based heritability estimates in 2 independent studies (total $N=913$ pairs) compared to non-centiled phenotypes (mean difference in h^2 estimates = 11.8%; Fig. 3C, SI6). In summary, centile normalisation of brain metrics reproducibly detects case-control and genetic influences on brain structure, as well as long-term sequelae of adverse birth outcomes even in the adult brain⁸.

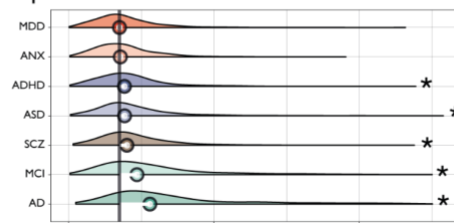
A| Median clinical centile difference to normative population



B| Centile Mahalanobis Distance



C| CMD across disorders



D| Centile heritability

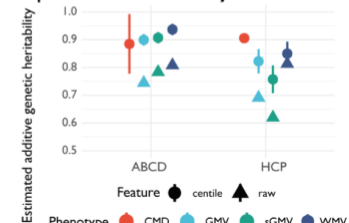


Fig. 3: Clinical differences and heritability of centile scores. A| Centile distributions for each of the clinical samples relative to the CN group median (depicted as a horizontal black line). The deviation in each clinical group is overlaid as a lollipop plot (white line with circle corresponding to the clinical group median). Pairwise tests for significance were done using Monte-Carlo permutation (10,000 permutations) and p-values adjusted using Benjamini-Hochberg FDR correction across all possible pairs. Only significant differences to CN (corrected $p < 0.001$) are depicted here and highlighted with an asterisk. For a complete overview of all pairwise comparisons, see SI 2.7 and SI tables 2 and 3. B| Schematic of summary measure of the Centile Mahalanobis Distance (CMD). CMD is a multivariate scaled distance summary of the four phenotypes listed in panel A, quantifying the total relative deviation of an individual from the CN group median. C| Probability density plots of CMD across disorders. Vertical black line depicts the median CMD of the CN group. Asterisks indicate an FDR-corrected significant difference from the CN group. D| Heritability of raw volumetric phenotypes and their reference-normalized centile scores across two twin studies. Abbreviations: Control (CN), Alzheimer's Disease (AD), Attention Deficit Hyperactivity Disorder (ADHD), Anxiety or Phobia (ANX), Autism Spectrum Disorder (ASD), Mild Cognitive Impairment (MCI), Major Depressive Disorder (MDD), Schizophrenia (SCZ); Gray Matter Volume (GMV), Subcortical Gray Matter Volume (sGMV), White Matter Volume (WMV), Centile Mahalanobis Distance (CMD).

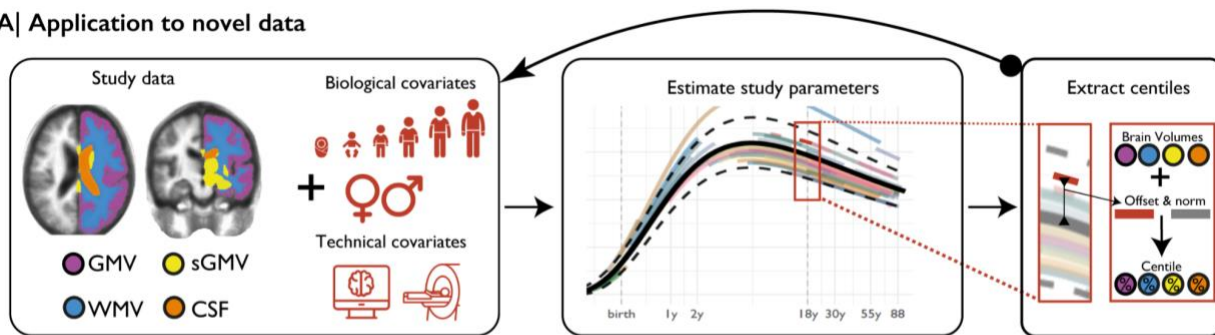
Longitudinal centile changes and novel data

Due to the relative paucity of longitudinal imaging (~10%), models were generated from single cross-sectional time points. However, the generalisability of cross-sectional models to longitudinal assessment is important for potential clinical utility. Intra-individual variability of derived centiles across longitudinal data, measured with the interquartile range (IQR), was low across both CN and clinical groups (all median <5%; SI1.6). Low intra-individual variability indicates a stable estimation across multiple sessions in general, although there is also evidence of inter-study and cross-disorder differences (SI9). Interestingly, individuals who changed diagnosis showed greater instability, for example there was higher IQR in individuals who progressed from CN to AD or MCI to AD (~5% median difference, corrected $P < 0.01$ across phenotypes; SI9 and SI Table 5). IQR was also slightly higher in younger samples (SI9). While the contribution of increased noise in earlier datasets due to the difficulties associated with scanning younger individuals cannot be

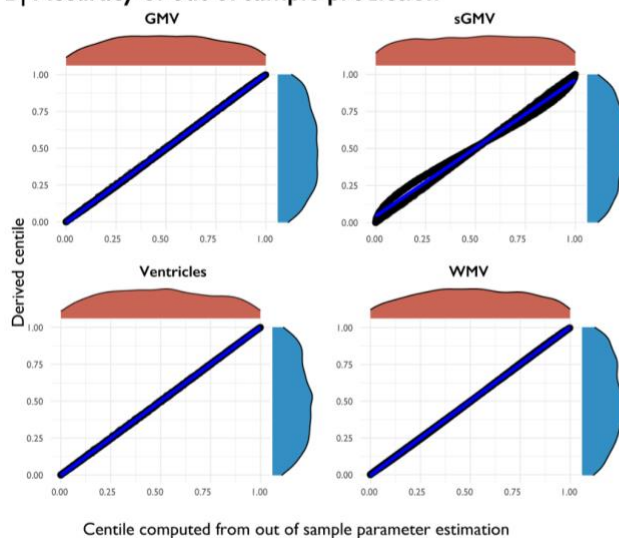
ruled out, higher IQR in early development is consistent with the idea of increased variability in periods of highly dynamic change observed across other anthropometric traits⁴⁰.

A key extension of the present growth charts is the estimation of centiles for data not included in the original models, requiring estimation of study-specific parameters. Thus, we implemented a maximum likelihood approach to estimate parameters for any new study not already included (Fig. 4A). This approach was tested on simulated data, 4 independent real-world datasets, and on data containing varying subsets of original data to estimate minimum sample size for robust normalisation (Fig. 4B-C, SI1.7). Centiles derived from parameter estimation and centiles derived when data were included (i.e. the full model was rerun) showed near perfect correspondence (all $R^2 > 0.99$). Jackknife and simulation analyses suggested that a minimum sample size of 100 provides robust estimation of mean and variance parameters combined. With 100+ subjects, the predicted study-centile confidence intervals fall within the range of the empirical confidence intervals (Fig. 4C, SI1.7).

A| Application to novel data



B| Accuracy of out of sample prediction



C| Minimum sample size

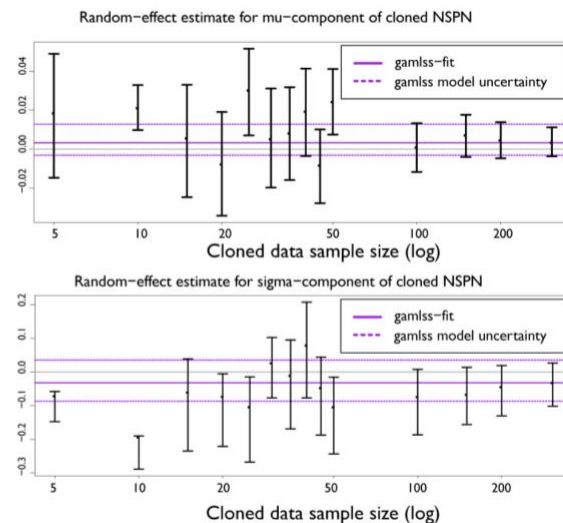


Fig. 4: Application to novel data. A| Schematic overview of the pipeline used for estimation of centile scores for novel data. Principally, maximum likelihood estimation is used to estimate the likely offset in novel studies relative to the established reference norms, and these estimated parameters are then used to derive individual centile scores. B| Scatter plots show the results from a real-world example of this procedure across 4 datasets not contained in the original model comprising ~2100 new subjects. Lines represent correlations between the centile scores as estimated via the maximum likelihood procedure (“Centile computed from out of sample parameter estimation”) versus as

estimated when including the studies in the reference models (“Derived centile”). Correlations are near-perfect in all cases ($R^2 > 0.99, P < 1-e16$). Supplementary section 1.7.2 shows the real-world example broken down by study. C|t Out-of-sample parameter estimation for the mu and sigma components of the GAMLSS model (SI 1). Vertical range plots show the outcomes after iterative increases in the sample size of independent hold-out datasets where the true parameter estimates and their confidence intervals are known (true values illustrated by horizontal purple lines).

The utility of brain reference charts

We have aggregated the largest neuroimaging dataset to date in an effort to modernise the concept of growth charts in the context of the human brain. We find that even at the macroscopic level of brain tissue classes, these standards show clear and robust clinical differences across multiple independent datasets. Their stability across longitudinal measurements and their ability to track documented changes in diagnoses bodes well for future predictive applications, especially as more longitudinal datasets become available⁴¹ and as early life data become more prevalent¹⁵. In particular, investigations of imaging-genetics relationships, such as associations with polygenic risk scores and genome-wide association studies⁴², may benefit from using centiles due to the increased heritability estimates from normalisation⁴³. Perhaps most importantly, centiles enable harmonisation across geographic and demographic profiles, and therefore can enrich the assessment of individual differences across clinical and behavioural domains⁴⁴. It should be stressed that the analogy to paediatric growth charts is not meant to imply a predetermined application for brain charts in a typical clinical setting – in the first instance, the utility of brain charts will be in the research context.

Another capacity of life-spanning centile scores is to enable direct comparisons between normative and clinical samples at different developmental stages. Notably, the effect sizes for metrics of premature birth were similar across samples spanning birth to 81 years. Moreover, the magnitude of centile differences in cortical gray matter and white matter in schizophrenia was comparable to that observed in AD, with largely non-overlapping age ranges. This result is consistent with the theory of mirrored neuroanatomical vulnerability in development and ageing, for example with late-to-develop brain areas being particularly susceptible to ageing-related atrophy⁴⁵. While brain imaging is part of the standard diagnostic work-up in dementia, with the ability to discriminate between pathological processes⁴⁶, our results underscore the potential diagnostic yield for a wider scope of human disease with the use of appropriate reference standards.

Inherent in the lifespan models is the ability to assess limitations in sample characteristics. Aggregated data revealed that fetal, neonatal and mid-adulthood (30-40yrs) epochs are underrepresented (Fig. 1A, SI Dataset Descriptions). Unfortunately, as is common in existing genetic datasets, ethnic and geographic representativeness was heavily biased towards European and North American samples. While our use of study-specific distribution parameters mitigates any geographic bias in centile scores, increasing inclusivity will strengthen population-representativeness^{47,48} and further strengthen out-of-sample estimation. The choice to stratify the lifespan models by sex was made based on the same logic as prior anthropometric growth charts: males have larger brain tissue volumes than females in absolute terms, but this difference is not associated with any difference in clinical or cognitive outcome. Future work aimed at directly

assessing sex-specific associations with centiles scores would also benefit from more detailed and dimensional self-report variables ^{49,50}.

As ongoing and future efforts provide increasing amounts of high quality data, we predict an iterative process of improved statistical models. While methodological (e.g., segmentation), theoretical (e.g., establishing regional homology across early developmental periods), and data sharing limitations directed our focus towards the major cerebral tissue classes, our models could also be adapted to integrate fine-grained regional measures and additional morphological features in future work. For the current set of reference charts, we provide interactive tools to explore existing models and to derive normalised centiles for new datasets across the lifespan at www.brainchart.io.

Acknowledgements

RAIB is supported by a British Academy Postdoctoral fellowship and Autism Research Trust. JS is supported by NIMH T32 MH019112-29 and K08MH120564. SRW was funded by UKRI Medical Research Council MC_UU_00002/2 and was supported by the NIHR Cambridge Biomedical Research Centre (BRC-1215-20014). ETB is supported by an NIHR Senior Investigator award. AFA-B is supported by NIMH K08MH120564. Data were curated and analysed using a computational facility funded by an MRC research infrastructure award ([MR/M009041/1](#)) and supported by the NIHR Cambridge Biomedical Research Centre. The views expressed are those of the authors and not necessarily those of the NIH, NHS, the NIHR or the Department of Health and Social Care. See supplementary materials for a comprehensive list of all contributing authors.

Disclosures

The authors have no conflicts of interest to disclose.

References

1. Cole, T. J. The development of growth references and growth charts. *Ann. Hum. Biol.* **39**, 382–394 (2012).
2. Paus, T., Keshavan, M. & Giedd, J. N. Why do many psychiatric disorders emerge during adolescence? *Nat. Rev. Neurosci.* **9**, 947–957 (2008).
3. Vigo, D., Thornicroft, G. & Atun, R. Estimating the true global burden of mental illness. *Lancet Psychiatry* **3**, 171–178 (2016).
4. Gertszolf, N. *et al.* Association between Subcortical Morphology and Cerebral White Matter

- Energy Metabolism in Neonates with Congenital Heart Disease. *Sci. Rep.* **8**, 14057 (2018).
5. Meuwly, E. *et al.* Postoperative brain volumes are associated with one-year neurodevelopmental outcome in children with severe congenital heart disease. *Sci. Rep.* **9**, 10885 (2019).
 6. Volpe, J. J. Brain injury in premature infants: a complex amalgam of destructive and developmental disturbances. *Lancet Neurol.* **8**, 110–124 (2009).
 7. Nosarti, C. *et al.* Preterm birth and psychiatric disorders in young adult life. *Arch. Gen. Psychiatry* **69**, E1–8 (2012).
 8. Wheeler, E. N. W. *et al.* Birth weight is associated with brain tissue volumes seven decades later, but not with age-associated changes to brain structure. *bioRxiv* 2020.08.27.270033 (2020) doi:10.1101/2020.08.27.270033.
 9. Jack, C. R., Jr *et al.* Tracking pathophysiological processes in Alzheimer’s disease: an updated hypothetical model of dynamic biomarkers. *Lancet Neurol.* **12**, 207–216 (2013).
 10. Heuer, K. & Toro, R. Role of mechanical morphogenesis in the development and evolution of the neocortex. *Phys. Life Rev.* **31**, 233–239 (2019).
 11. Werling, D. M. *et al.* Whole-Genome and RNA Sequencing Reveal Variation and Transcriptomic Coordination in the Developing Human Prefrontal Cortex. *Cell Rep.* **31**, 107489 (2020).
 12. Gilmore, J. H., Knickmeyer, R. C. & Gao, W. Imaging structural and functional brain development in early childhood. *Nat. Rev. Neurosci.* **19**, 123–137 (2018).
 13. Gandal, M. J., Leppa, V., Won, H., Parikshak, N. N. & Geschwind, D. H. The road to precision psychiatry: translating genetics into disease mechanisms. *Nat. Neurosci.* **19**, 1397–1407 (2016).
 14. Opel, N. *et al.* Cross-Disorder Analysis of Brain Structural Abnormalities in Six Major Psychiatric Disorders: A Secondary Analysis of Mega- and Meta-analytical Findings From the ENIGMA Consortium. *Biol. Psychiatry* **88**, 678–686 (2020).

15. Howell, B. R. *et al.* The UNC/UMN Baby Connectome Project (BCP): An overview of the study design and protocol development. *Neuroimage* **185**, 891–905 (2019).
16. Bycroft, C. *et al.* The UK Biobank resource with deep phenotyping and genomic data. *Nature* **562**, 203–209 (2018).
17. Garavan, H. *et al.* Recruiting the ABCD sample: Design considerations and procedures. *Dev. Cogn. Neurosci.* **32**, 16–22 (2018).
18. Zöllei, L., Iglesias, J. E., Ou, Y., Grant, P. E. & Fischl, B. Infant FreeSurfer: An automated segmentation and surface extraction pipeline for T1-weighted neuroimaging data of infants 0-2 years. *Neuroimage* **218**, 116946 (2020).
19. Stasinopoulos, D. & Rigby, R. Generalized Additive Models for Location Scale and Shape (GAMLSS) in R. *Journal of Statistical Software, Articles* **23**, 1–46 (2007).
20. Borghi, E. *et al.* Construction of the World Health Organization child growth standards: selection of methods for attained growth curves. *Stat. Med.* **25**, 247–265 (2006).
21. Knickmeyer, R. C. *et al.* A structural MRI study of human brain development from birth to 2 years. *J. Neurosci.* **28**, 12176–12182 (2008).
22. Gilmore, J. H. *et al.* Individual Variation of Human Cortical Structure Is Established in the First Year of Life. *Biol Psychiatry Cogn Neurosci Neuroimaging* **5**, 971–980 (2020).
23. Courchesne, E. *et al.* Normal brain development and aging: quantitative analysis at in vivo MR imaging in healthy volunteers. *Radiology* **216**, 672–682 (2000).
24. Narvacan, K., Treit, S., Camicioli, R., Martin, W. & Beaulieu, C. Evolution of deep gray matter volume across the human lifespan. *Hum. Brain Mapp.* **38**, 3771–3790 (2017).
25. Ritchie, S. J. *et al.* Sex Differences in the Adult Human Brain: Evidence from 5216 UK Biobank Participants. *Cereb. Cortex* **28**, 2959–2975 (2018).
26. Tanner, J. M. *Growth at adolescence*, 2nd ed. **2**, (1962).
27. Bozzola, M. & Meazza, C. Growth Velocity Curves: What They Are and How to Use Them. *Handbook of Growth and Growth Monitoring in Health and Disease* 2999–3011 (2012)

doi:10.1007/978-1-4419-1795-9_180.

28. Tanner, J. M., Whitehouse, R. H. & Takaishi, M. Standards from birth to maturity for height, weight, height velocity, and weight velocity: British children, 1965. I. *Arch. Dis. Child.* **41**, 454–471 (1966).
29. Holland, D. *et al.* Structural growth trajectories and rates of change in the first 3 months of infant brain development. *JAMA Neurol.* **71**, 1266–1274 (2014).
30. Tau, G. Z. & Peterson, B. S. Normal development of brain circuits. *Neuropsychopharmacology* **35**, 147–168 (2010).
31. Huttenlocher, P. R. & Dabholkar, A. S. Regional differences in synaptogenesis in human cerebral cortex. *J. Comp. Neurol.* **387**, 167–178 (1997).
32. Petanjek, Z. *et al.* Extraordinary neoteny of synaptic spines in the human prefrontal cortex. *Proc. Natl. Acad. Sci. U. S. A.* **108**, 13281–13286 (2011).
33. Miller, D. J. *et al.* Prolonged myelination in human neocortical evolution. *Proc. Natl. Acad. Sci. U. S. A.* **109**, 16480–16485 (2012).
34. Blüml, S. *et al.* Metabolic maturation of the human brain from birth through adolescence: insights from in vivo magnetic resonance spectroscopy. *Cereb. Cortex* **23**, 2944–2955 (2013).
35. Kuzawa, C. W. *et al.* Metabolic costs and evolutionary implications of human brain development. *Proc. Natl. Acad. Sci. U. S. A.* **111**, 13010–13015 (2014).
36. WHO MULTICENTRE GROWTH REFERENCE STUDY GROUP & Onis, M. WHO Motor Development Study: Windows of achievement for six gross motor development milestones. *Acta Paediatr.* **95**, 86–95 (2007).
37. Kang, H. J. *et al.* Spatio-temporal transcriptome of the human brain. *Nature* **478**, 483–489 (2011).
38. Gur, R. E. *et al.* Reduced dorsal and orbital prefrontal gray matter volumes in schizophrenia. *Arch. Gen. Psychiatry* **57**, 761–768 (2000).

39. Andreasen, N. C. *et al.* Progressive brain change in schizophrenia: a prospective longitudinal study of first-episode schizophrenia. *Biol. Psychiatry* **70**, 672–679 (2011).
40. Sorva, R., Lankinen, S., Tolppanen, E. M. & Perheentupa, J. Variation of growth in height and weight of children. II. After infancy. *Acta Paediatr. Scand.* **79**, 498–506 (1990).
41. Alcohol Research: Current Reviews Editorial Staff. NIH’s Adolescent Brain Cognitive Development (ABCD) Study. *Alcohol Res.* **39**, 97 (2018).
42. Elliott, L. T. *et al.* Genome-wide association studies of brain imaging phenotypes in UK Biobank. *Nat. Neurosci.* **562**, 210–216 (2018).
43. Kochunov, P. *et al.* Homogenizing Estimates of Heritability Among SOLAR-Eclipse, OpenMx, APACE, and FPHI Software Packages in Neuroimaging Data. *Front. Neuroinform.* **13**, 16 (2019).
44. Marquand, A. F., Rezek, I., Buitelaar, J. K. & Beckmann, C. F. Understanding Heterogeneity in Clinical Cohorts Using Normative Models: Beyond Case-Control Studies. *Biol. Psychiatry* **80**, 552–561 (2016).
45. Tamnes, C. K. *et al.* Brain development and aging: overlapping and unique patterns of change. *Neuroimage* **68**, 63–74 (2013).
46. Staffaroni, A. M. *et al.* Neuroimaging in Dementia. *Semin. Neurol.* **37**, 510–537 (2017).
47. Dong, H.-M. *et al.* Charting brain growth in tandem with brain templates at school age. *Sci. Bull.* **65**, 1924–1934 (2020).
48. Sharma, E. *et al.* Consortium on Vulnerability to Externalizing Disorders and Addictions (cVEDA): A developmental cohort study protocol. *BMC Psychiatry* **20**, 2 (2020).
49. Clayton, J. A. & Tannenbaum, C. Reporting Sex, Gender, or Both in Clinical Research? *JAMA* **316**, 1863–1864 (2016).
50. Shansky, R. M. & Murphy, A. Z. Considering sex as a biological variable will require a global shift in science culture. *Nat. Neurosci.* **24**, 457–464 (2021).

Online methods: Brain charts for the human lifespan

To accurately and comprehensively establish standardised brain reference charts across the lifespan, it is crucial to leverage multiple independent and diverse datasets, especially those spanning prenatal and early postnatal life. Here we sought to chart normative brain development and ageing across the largest age-span and largest aggregated neuroimaging dataset to date using a robust and scalable methodological framework ^{1,2}. We leveraged these normative reference charts in clinical cohorts to generate individualised assessments of age-relative centiles. These centiles were then leveraged to investigate cross-diagnostic and longitudinal atypicalities of brain morphology across the lifespan. We used generalised additive models for location scale and shape (GAMLSS) ¹ to estimate cross-sectional normative age-related trends (supplementary information [SI]) from 75,241 individuals without neuropsychiatric conditions from 96 studies (see supplementary tables T1.1-T1.6 for full demographic information and SI Dataset Descriptions). The GAMLSS approach allows not only or age-related changes in average brain size but also age related-changes in the variability of brain size, in the form of both linear and nonlinear changes over time, thereby overcoming potential limitations of conventional additive models that only allow additive means to be modelled ¹. In addition, site-specific offsets in estimates of average brain size and variability in brain size are also modelled. These modelling criteria are particularly important in the context of establishing growth references as recommended by the World Health Organisation ², as it is reasonable to assume the distribution of higher order moments (e.g. variance) changes with age, sex, site and pre-processing pipeline - especially given the impossibility of fully comprehensive longitudinal data for individuals spanning the ~100 year age range. Furthermore, recent studies suggest that changes in across-individual variability might intersect with vulnerability for developing a mental health condition ³. The use of data spanning the entire age range is also critical, as estimation from partial age-windows can lead to biased estimations when extrapolated to the whole lifespan. In summary, using a sex-stratified approach ², age, preprocessing pipeline and study were each included in the GAMLSS model estimation of first order (μ) and second order (σ) distribution parameters of a generalised gamma distribution using fractional polynomial to model nonlinear trends. See Supplemental Methods for further details.

In general, the GAMLSS framework can be specified in the following way:

$$\begin{aligned} Y &\sim D(\mu, \sigma, \nu, \tau), \\ g_\mu(\mu) &= X_\mu\beta_\mu + Z_\mu\gamma_\mu + \sum_i s_{\mu,i}(x_i), \\ g_\sigma(\sigma) &= X_\sigma\beta_\sigma + Z_\sigma\gamma_\sigma + \sum_i s_{\sigma,i}(x_i), \\ g_\nu(\nu) &= X_\nu\beta_\nu + Z_\nu\gamma_\nu + \sum_i s_{\nu,i}(x_i), \\ g_\tau(\tau) &= X_\tau\beta_\tau + Z_\tau\gamma_\tau + \sum_i s_{\tau,i}(x_i). \end{aligned}$$

Here, the outcome vector, Y , follows a probability distribution D parameterised by up to four parameters, (μ, σ, ν, τ) . The four parameters, depending on the parameterisation of the probability density function, may correspond to the mean, variance, skewness, and kurtosis (i.e. the first four moments); however, for many distributions there is not a direct one-to-one correspondence. Each

component is linked to a linear equation through a link-function, $g(\cdot)$, and each component equation may include three types of terms: fixed effects, β (with design matrix, X); random-effects, γ (with design matrix, Z); and non-parametric smoothing functions, $s_{\cdot i}$ applied to the i^{th} covariate. The nature of the outcome distribution determines the appropriate link-functions and which components are used. In principle any outcome distribution can be used, from well-behaved continuous and discrete outcomes, through to mixtures and truncations.

Within this paper we consider fractional polynomials as a flexible, yet limited in complexity, approach to modelling age-related changes. Although non-parametric smoothers are more flexible, they can become unstable and infeasible, especially in the presence of random-effects. Hence, the fractional polynomials enter the model within the X terms, with associated coefficients in β . The GAMLSS framework includes the ability to estimate the most appropriate powers within the iterative fitting algorithm, searching across the standard set of powers, $p \in \{-2, -1, -0.5, 0, 0.5, 1, 2, 3\}$, where the design matrix includes the covariate (in our setting, age) raised to the power, namely, x^p . Fractional polynomials naturally extend to higher-orders, for example a second-order fractional polynomial of the form, $x^{p_1} + x^{p_2}$.

There are several options for including random-effects within the GAMLSS framework depending on the desired covariance structures. We consider the simplest case, including a factor-level (or group-level) random-intercept, where the observations are grouped by the study covariate. The random-effects are drawn from a normal distribution with zero mean and variance to be estimated, $\gamma \sim N(0, \delta^2)$. The ability to include random-effects is fundamental to accounting for co-dependence between observations. It is therefore possible to take advantage of the flexibility of "standard" GAMLSS, as typically used to develop growth charts^{2,4,5}, while accounting for co-dependence between observations using random-effects. The typical applications of GAMLSS assume independent and identically distributed outcomes; however within our context it is essential to account for within-study covariance implying the observations are no longer independent.

This model allowed us to leverage the aggregated life-spanning neuroimaging dataset to derive developmental milestones (i.e., peaks of trajectories) and compare them to existing literature. Peaks were determined based on the GAMLSS model output (50th centile) for each of the tissue classes and TCv, for both total volumes (Fig. 1B) and rates of change or growth ("velocity"; Fig. 1E). Diagnostic age ranges from previous literature^{6,7} were plotted (black boxes in Fig. 2) to compare with empirical age ranges of patients with a given diagnosis across the aggregated neuroimaging dataset. Note that age of diagnosis is significantly later than age of symptom onset for many disorders⁶. Developmental milestones were re-plotted from published work for brain resting metabolic rate (RMR)⁸, anthropometric variables⁹, and typical acquisition of the six gross motor capabilities⁴. Pubertal age ranges were taken from reported typical age ranges^{10,11}.

Furthermore, these neuroimaging-derived brain reference charts also enabled each individual to be quantified relative to a statistical distribution defined at the reference level for any point during the lifespan^{12,13}. Individual centile scores were obtained relative to the reference curves, conceptually similar to traditional anthropometric growth charts. These normative scores

represent a novel set of population and age standardized clinical phenotypes, providing the capacity for cross-phenotype, cross-study and cross-disorder comparison. A single summary deviation metric for each individual was also generated.. Main group effects were analysed with a bootstrapped (500 bootstraps) non-parametric generalisation of Welch's one-way ANOVA. Pairwise, sex stratified, post-hoc comparisons were conducted using non-parametric Monte-Carlo permutation tests (10,000 permutations) and thresholded at a Benjamini-Hochberg false discovery rate (FDR) of $q < 0.05$.

To utilise the centiles in a diagnostically meaningful or predictive way, they need to be stable across multiple measuring points. To assess this intra-individual stability, we calculated the subject specific interquartile range (IQR) of centiles across timepoints for the datasets that included longitudinal scans ($n = 9,306$, 41 unique studies). Exploratory longitudinal clinical analyses were restricted to clinical groups that had at least 50 subjects with longitudinal data to allow for robust group-wise estimates of longitudinal variability. In addition, there was a small subset of individuals with documented pathological progression across longitudinal scans, for instance from high-risk status to formal diagnosis. Here, we would expect an associated change in centile measurement. To test this hypothesis, we assessed whether these individuals showed differences in centile variability (as assessed with IQR), and their approximate direction of change.

Finally, we provide an interactive tool (www.brainchart.io) and have made our code and models openly available (<https://github.com/ucam-department-of-psychiatry/Lifespan>). The tool not only allows the user to visualise the underlying datasets' demographics and reported reference charts in a much more detailed fashion than static images allow, it also provides the opportunity for interactive exploration of differences in centile scores across many clinical groups that is beyond the present manuscript. Perhaps most significantly, it includes an out-of-sample estimator of model parameters for novel data that enables the user to compute percentile scores for their own datasets without the computational or data-sharing hurdles involved in adding that data to the reference chart. All modelling included extensive validation, sensitivity analyses and multi-modal validation against existing growth chart references .

Though already based on the largest and most comprehensive neuroimaging dataset to date and supporting analyses of out-of-sample data , the underlying reference charts will also be updated as additional data is made available.

Methods References

1. Stasinopoulos, D. & Rigby, R. Generalized Additive Models for Location Scale and Shape (GAMLSS) in R. *Journal of Statistical Software, Articles* **23**, 1–46 (2007).
2. Borghi, E. *et al.* Construction of the World Health Organization child growth standards: selection of methods for attained growth curves. *Stat. Med.* **25**, 247–265 (2006).
3. Wierenga, L. M. *et al.* Greater male than female variability in regional brain structure across

- the lifespan. *Hum. Brain Mapp.* (2020) doi:10.1002/hbm.25204.
4. WHO MULTICENTRE GROWTH REFERENCE STUDY GROUP & Onis, M. WHO Motor Development Study: Windows of achievement for six gross motor development milestones. *Acta Paediatr.* **95**, 86–95 (2007).
 5. Heude, B. *et al.* A big-data approach to producing descriptive anthropometric references: a feasibility and validation study of paediatric growth charts. *Lancet Digit Health* **1**, e413–e423 (2019).
 6. Solmi, M. *et al.* Age at onset of mental disorders worldwide: large-scale meta-analysis of 192 epidemiological studies. *Mol. Psychiatry* 1–15 (2021).
 7. Erkkinen, M. G., Kim, M.-O. & Geschwind, M. D. Clinical Neurology and Epidemiology of the Major Neurodegenerative Diseases. *Cold Spring Harb. Perspect. Biol.* **10**, (2018).
 8. Kuzawa, C. W. *et al.* Metabolic costs and evolutionary implications of human brain development. *Proc. Natl. Acad. Sci. U. S. A.* **111**, 13010–13015 (2014).
 9. Bozzola, M. & Meazza, C. Growth Velocity Curves: What They Are and How to Use Them. *Handbook of Growth and Growth Monitoring in Health and Disease* 2999–3011 (2012) doi:10.1007/978-1-4419-1795-9_180.
 10. Tanner, J. M., Whitehouse, R. H. & Takaishi, M. Standards from birth to maturity for height, weight, height velocity, and weight velocity: British children, 1965. I. *Arch. Dis. Child.* **41**, 454–471 (1966).
 11. Tanner, J. M. Growth at adolescence, 2nd ed. **2**, (1962).
 12. Marquand, A. F., Rezek, I., Buitelaar, J. K. & Beckmann, C. F. Understanding Heterogeneity in Clinical Cohorts Using Normative Models: Beyond Case-Control Studies. *Biol. Psychiatry* **80**, 552–561 (2016).
 13. Bethlehem, R. A. I. *et al.* A normative modelling approach reveals age-atypical cortical thickness in a subgroup of males with autism spectrum disorder. *Commun Biol* **3**, 486 (2020).

Affiliations

- ¹ Autism Research Centre, Department of Psychiatry, University of Cambridge, Cambridge, CB2 0SZ, UK.
- ² Brain Mapping Unit, Department of Psychiatry, University of Cambridge, Cambridge, CB2 0SZ, UK
- ³ Department of Psychiatry, University of Pennsylvania, Philadelphia, PA 19104
- ⁴ Department of Child and Adolescent Psychiatry and Behavioral Science, The Children's Hospital of Philadelphia, Philadelphia, PA 19104
- ⁵ Department of Psychiatry, University of Cambridge, Cambridge, CB2 0SZ, UK
- ⁶ MRC Biostatistics Unit, University of Cambridge, Cambridge, England
- ⁷ Lifespan Informatics & Neuroimaging Center, University of Pennsylvania, Philadelphia, PA 19104
- ⁸ Department of Psychology, Yale University, New Haven, CT, USA
- ⁹ Developmental Imaging, Murdoch Children's Research Institute, Melbourne, Victoria, Australia
- ¹⁰ Department of Medicine, Monash University, Melbourne, Victoria, Australia
- ¹¹ UCL Great Ormond Street Institute for Child Health, 30 Guilford St, Holborn, London WC1N 1EH
- ¹² Weill Cornell Institute of Geriatric Psychiatry, Department of Psychiatry, Weill Cornell Medicine
- ¹³ Department of Pediatrics University of Toronto
- ¹⁴ Holland Bloorview Kids Rehabilitation Hospital, Toronto, Canada
- ¹⁵ Joint China-Cuba Lab, University of Electronic Science and Technology, Chengdu China/Cuban Center for Neuroscience, La Habana, Cuba
- ¹⁶ MRC Cognition and Brain Sciences Unit, University of Cambridge, Cambridge UK
- ¹⁷ Department of Psychology, School of Philosophy, Psychology and Language Sciences, University of Edinburgh, Edinburgh, United Kingdom
- ¹⁸ University College London, Mental Health Neuroscience Research Department, Division of Psychiatry, London UK
- ¹⁹ Department of Paediatrics, University of Melbourne, Melbourne, Victoria, Australia
- ²⁰ Cambridge Lifetime Asperger Syndrome Service (CLASS), Cambridgeshire and Peterborough NHS Foundation Trust, Cambridge, United Kingdom
- ²¹ Centre for Addiction Medicine, National Institute of Mental Health and Neurosciences, Bengaluru, India 560029
- ²² Department of Neurology, Max Planck Institute for Human Cognitive and Brain Sciences, Leipzig, 04103, Germany
- ²³ Department of Neuropsychiatry, Seoul National University Bundang Hospital, Seongnam, Korea
- ²⁴ Department of Human Genetics, South Texas Diabetes and Obesity Institute, University of Texas Rio Grande Valley
- ²⁵ MRC Centre for Reproductive Health, University of Edinburgh, UK
- ²⁶ Fetal and Neonatal Institute, Division of Neonatology, Children's Hospital Los Angeles, Department of Pediatrics, Keck School of Medicine, University of Southern California, Los Angeles, California USA
- ²⁷ McGill Centre for Integrative Neuroscience, Ludmer Centre for Neuroinformatics and Mental Health, Montreal Neurological Institute
- ²⁸ McGill University
- ²⁹ Department of Brain Sciences, Imperial College London, London UK & Care Research & Technology Centre, UK Dementia Research Institute
- ³⁰ Tri-institutional Center for Translational Research in Neuroimaging and Data Science, Georgia State University, Georgia Institute of Technology, and Emory University, Atlanta, GA, USA
- ³¹ Computational Brain Anatomy (CoBra) Laboratory, Cerebral Imaging Centre, Douglas Mental Health University Institute
- ³² Penn Statistics in Imaging and Visualization Center, Department of Biostatistics, Epidemiology, and Informatics, Perelman School of Medicine, University of Pennsylvania, Philadelphia, PA, USA
- ³³ Normandie Univ, UNICAEN, INSERM, U1237, PhIND "Physiopathology and Imaging of Neurological Disorders", Institut Blood and Brain @ Caen-Normandie, Cyceron, 14000 Caen, France
- ³⁴ Singapore Institute for Clinical Sciences, Agency for Science, Technology and Research, Singapore
- ³⁵ Department of Obstetrics and Gynaecology, Yong Loo Lin School of Medicine, National University of Singapore, Singapore
- ³⁶ Centre for Medical Image Computing (CMIC), University College London
- ³⁷ Dementia Research Centre (DRC), University College London

- ³⁸ Department of Psychiatry, Trinity College, Dublin, Ireland
- ³⁹ Department of Neuroscience, University of California, San Diego, San Diego, CA 92093, USA
- ⁴⁰ Autism Center of Excellence, University of California, San Diego, San Diego, CA 92037, USA
- ⁴¹ Institute of Neurodegenerative Disorders, CNRS UMR5293, University of Bordeaux
- ⁴² Melbourne Neuropsychiatry Centre, University of Melbourne, Melbourne, Australia
- ⁴³ The Hospital for Sick Children, Toronto, Canada
- ⁴⁴ Department of Psychiatry, School of Medicine, Pontificia Universidad Católica de Chile, Diagonal Paraguay 362, Santiago 8330077, Chile
- ⁴⁵ Department of Psychosis Studies, Institute of Psychiatry, Psychology and Neuroscience, King's College London, De Crespigny Park, London SE5 8AF, UK
- ⁴⁶ UNICAEN, INSERM, U1237, PHIND "Physiopathology and Imaging of Neurological Disorders", Institut Blood and Brain @ Caen-Normandie, Cyceron, 14000 Caen, France
- ⁴⁷ Social, Genetic and Developmental Psychiatry Centre, Institute of Psychiatry, Psychology & Neuroscience, King's College London, London, United Kingdom
- ⁴⁸ Cerebral Imaging Centre, Douglas Mental Health University Institute, Montreal, QC, Canada
- ⁴⁹ Department of Psychiatry, McGill University, Montreal, QC, Canada
- ⁵⁰ Department of Psychiatry, Brigham and Women's Hospital, Harvard Medical School, Boston, Massachusetts, United States
- ⁵¹ Max Planck UCL Centre for Computational Psychiatry and Ageing Research, University College London, London, UK.
- ⁵² Wellcome Centre for Human Neuroimaging, University College London, London, UK
- ⁵³ University of Cape Town, South Africa, Cape Town, South Africa
- ⁵⁴ Center for Neuroimaging, Cognition & Genomics (NICOG), School of Psychology, National University of Ireland Galway, Galway, Ireland
- ⁵⁵ Weil Family Brain and Mind Research Institute, Department of Psychiatry, Weill Cornell Medicine
- ⁵⁶ Centre for the Developing Brain, King's College London, London, UK
- ⁵⁷ Evelina London Children's Hospital
- ⁵⁸ Institute of Child Development, Department of Pediatrics, Masonic Institute for the Developing Brain, University of Minnesota, Minneapolis, MN, United States
- ⁵⁹ Department of Psychiatry, Center for Behavior Genetics of Aging, University of California, San Diego, La Jolla, CA
- ⁶⁰ Desert-Pacific Mental Illness Research Education and Clinical Center, VA San Diego Healthcare, San Diego, CA, USA
- ⁶¹ Department of Psychiatry, University of California San Diego, Los Angeles, CA, USA
- ⁶² Department of Psychiatry, University of Cambridge, and Wellcome Trust MRC Institute of Metabolic Science, Cambridge Biomedical Campus, Cambridge, United Kingdom
- ⁶³ Cambridgeshire and Peterborough NHS Foundation Trust
- ⁶⁴ Department of Clinical, Educational and Health Psychology, University College London, London, UK
- ⁶⁵ Department of Psychiatry, Center for Behavior Genetics of Aging, University of California, San Diego, La Jolla, CA 92093
- ⁶⁶ Cuban Center for Neuroscience, La Habana, Cuba
- ⁶⁷ Computational Radiology Laboratory, Boston Children's Hospital, Boston, MA 02115
- ⁶⁸ Department of Child and Adolescent Psychiatry, University of California, San Diego, San Diego, CA 92093, USA
- ⁶⁹ Department of Psychiatry, University of North Carolina, Chapel Hill, NC, USA
- ⁷⁰ Department of Psychiatry, Boston Children's Hospital and Harvard Medical School, Boston, MA 02115
- ⁷¹ Harvard Medical School, Boston, MA 02115
- ⁷² Division of Newborn Medicine and Neuroradiology, Fetal Neonatal Neuroimaging and Developmental Science Center, Boston Children's Hospital, Harvard Medical School, Boston, MA 02115, USA
- ⁷³ Department of Paediatrics and Child Health, Red Cross War Memorial Children's Hospital, SA-MRC Unit on Child & Adolescent Health, University of Cape Town, South Africa
- ⁷⁴ Neuroscience Institute, University of Cape Town, Cape Town, South Africa
- ⁷⁵ Lifespan Brain Institute, The Children's Hospital of Philadelphia, Philadelphia, PA 19104
- ⁷⁶ Lifespan Brain Institute, The Children's Hospital of Philadelphia, Philadelphia, PA 19105
- ⁷⁷ Mouse Imaging Centre, Toronto, Canada
- ⁷⁸ Clinical Memory Research Unit, Department of Clinical Sciences Malmö, Lund University, Malmö, Sweden

- ⁷⁹ Memory Clinic, Skåne University Hospital, Malmö, Sweden
- ⁸⁰ Department of Neurology, Icahn School of Medicine at Mount Sinai, New York, NY 10029, USA
- ⁸¹ Athinoula A. Martinos Center for Biomedical Imaging, Department of Radiology, Massachusetts General Hospital, Harvard Medical School, Boston, MA 02129, USA
- ⁸² Department of Psychiatry and Psychotherapy, Charite University Hospital Berlin, Berlin, Germany
- ⁸³ Department of Psychiatry, University of Cambridge, Cambridge, UK
- ⁸⁴ Department of Neuropsychology, Max Planck Institute for Human Cognitive and Brain Sciences, Leipzig, Germany
- ⁸⁵ Université de Paris, Paris, France
- ⁸⁶ Department of Psychiatry, University of Cape Town, Cape Town, South Africa.
- ⁸⁷ Departments of Psychiatry and Integrative Medicine, NIMHANS, Bengaluru, India
- ⁸⁸ Departments of Psychology and Psychiatry, Yale University, New Haven, CT, USA
- ⁸⁹ Radiology Research, Children's Hospital of Philadelphia, Philadelphia, United States
- ⁹⁰ The Department of Radiology, Perelman School of Medicine, University of Pennsylvania, Philadelphia, United States
- ⁹¹ Division of Newborn Medicine, Fetal Neonatal Neuroimaging and Developmental Science Center, Boston Children's Hospital, Harvard Medical School, Boston, MA 02115, USA
- ⁹² Boston Children's Hospital, Boston, MA 02115
- ⁹³ Department of Psychiatry and Mental Health, Clinical Neuroscience Institute, University of Cape Town
- ⁹⁴ Department of Radiology, Mayo Clinic, Rochester, MN 55905, USA
- ⁹⁵ Department of Psychiatry, Universidade Federal de São Paulo
- ⁹⁶ National Institute of Developmental Psychiatry, CNPq
- ⁹⁷ Institute of Science and Technology for Brain-Inspired Intelligence, Fudan University, Shanghai, 200433, China
- ⁹⁸ Key Laboratory of Computational Neuroscience and BrainInspired Intelligence (Fudan University), Ministry of Education, Shanghai, China
- ⁹⁹ Centre for Population Neuroscience and Precision Medicine (PONNS), Institute of Psychiatry, Psychology and Neuroscience, SGDP Centre, King's College London, London SE5 8AF, UK
- ¹⁰⁰ Harvard Aging Brain Study, Department of Neurology, Massachusetts General Hospital, Boston, MA 02114
- ¹⁰¹ Center for Alzheimer Research and Treatment, Department of Neurology, Brigham and Women's Hospital, Boston, MA 02115
- ¹⁰² Department of Radiology, Massachusetts General Hospital, Boston, MA
- ¹⁰³ Cambridgeshire and Peterborough NHS Foundation Trust, Huntingdon, United Kingdom
- ¹⁰⁴ Department of Neurology, Mayo Clinic, Rochester, MN, USA
- ¹⁰⁵ Department of Radiology, Mayo Clinic, Rochester, MN, USA
- ¹⁰⁶ Department of Psychiatry Division of Neurosciences, University Medical Center, Utrecht, The Netherlands
- ¹⁰⁷ Department of Psychiatry, Icahn School of Medicine, Mount Sinai, New York, USA
- ¹⁰⁸ Department of Clinical Medicine, Department of Psychiatry and Turku Brain and Mind Center, FinnBrain Birth Cohort Study, University of Turku and Turku University Hospital, Turku, Finland
- ¹⁰⁹ Centre for Population Health Research, Turku University Hospital and University of Turku, Turku, Finland
- ¹¹⁰ Turku Brain and Mind Center, Department of Clinical Medicine
- ¹¹¹ Institute of Development, Aging and Cancer, Tohoku University, Seiryochō, Aobaku, Sendai 980-8575, Japan
- ¹¹² Queen's University, Department of Psychology, Centre for Neuroscience Studies, Kingston, Ontario, Canada
- ¹¹³ Institute of Neuroscience and Physiology, University of Gothenburg, Gothenburg, Sweden
- ¹¹⁴ Department of Brain and Cognitive Sciences, Seoul National University College of Natural Sciences, Seoul, Republic of Korea
- ¹¹⁵ Department of Neuropsychiatry, Seoul National University Bundang Hospital, Seongnam, Republic of Korea
- ¹¹⁶ Department of Psychiatry, Seoul National University College of Medicine, Seoul, Republic of Korea
- ¹¹⁷ Section on Developmental Neurogenomics, Human Genetics Branch, National Institute of Mental Health, Bethesda, MD, USA
- ¹¹⁸ Department of Brain & Cognitive Sciences, Seoul National University College of Natural Sciences, Seoul, Korea
- ¹¹⁹ Department of Medical Biophysics, University of Toronto, Toronto, ON, Canada
- ¹²⁰ Mouse Imaging Centre, The Hospital for Sick Children, Toronto, ON, Canada
- ¹²¹ Wellcome Centre for Integrative Neuroimaging, FMRIB, Nuffield Department of Clinical Neuroscience, University of Oxford, Oxford, UK
- ¹²² Montreal Neurological Institute, McGill University, Montreal, Canada

- ¹²³ The Clinical Hospital of Chengdu Brain Science Institute, University of Electronic Science and Technology of China, Chengdu 611731, China
- ¹²⁴ Department of Psychiatry and Brain and Mind Research Institute, Weill Cornell Medicine
- ¹²⁵ Laboratory for Autism and Neurodevelopmental Disorders, Center for Neuroscience and Cognitive Systems @UniTn, Istituto Italiano di Tecnologia, Rovereto, Italy
- ¹²⁶ School of Biomedical Engineering & Brain and Mind Centre, The University of Sydney, Sydney, NSW, Australia
- ¹²⁷ Department of Psychology, University of Texas, Austin, Texas 78712, USA
- ¹²⁸ Department of Psychiatry and Neuropsychology, School of Mental Health and Neuroscience, EURON, Maastricht University Medical Centre, PO Box 616, 6200 MD, Maastricht, the Netherlands; Institute for Mental Health Care Eindhoven (GGzE), Eindhoven, the Netherlands.
- ¹²⁹ McConnell Brain Imaging Centre, Montreal Neurological Institute, McGill University, Montreal, QC H3A 2B4, Canada
- ¹³⁰ Bordeaux University Hospital
- ¹³¹ Professor, Department of Psychosis Studies, Institute of Psychiatry, Psychology and Neuroscience, King's College London, UK
- ¹³² Ludmer Centre for Neuroinformatics and Mental Health, Douglas Mental Health University Institute, McGill University, Montreal, Quebec, Canada; Singapore Institute for Clinical Sciences, Singapore
- ¹³³ Department of Computer Science and Technology, University of Cambridge, Cambridge CB3 0FD, United Kingdom
- ¹³⁴ Department of Psychiatry, University of Cambridge, Cambridge CB2 0SZ, United Kingdom
- ¹³⁵ The Alan Turing Institute, London, NW1 2DB
- ¹³⁶ Department of Psychology, School of Business, National College of Ireland, Dublin, Ireland
- ¹³⁷ School of Psychology & Center for Neuroimaging and Cognitive Genomics, National University of Ireland Galway, Galway, Ireland
- ¹³⁸ Department of Psychiatry, Trinity College Dublin, Dublin, Ireland
- ¹³⁹ Department of Psychiatry, School of Medicine, Oregon Health and Science University, Portland, United States
- ¹⁴⁰ Center for Sleep and Cognition, Yong Loo Lin School of Medicine, National University of Singapore, Singapore
- ¹⁴¹ Department of Pediatrics, Washington University in St. Louis, St. Louis, Missouri, United States
- ¹⁴² Alzheimer Center Amsterdam, Department of Neurology, Amsterdam Neuroscience, Vrije Universiteit Amsterdam, Amsterdam UMC, Amsterdam, The Netherlands
- ¹⁴³ Lund University, Clinical Memory Research Unit, Lund, Sweden
- ¹⁴⁴ Robarts Research Institute & The Brain and Mind Institute, University of Western Ontario, London, Ontario, Canada.
- ¹⁴⁵ INSERM, U1237, PhIND "Physiopathology and Imaging of Neurological Disorders", Institut Blood and Brain @ Caen-Normandie, Cyceron, 14000 Caen, France
- ¹⁴⁶ Department of Psychiatry, Federal University of Sao Paulo (UNIFESP)
- ¹⁴⁷ National Institute of Developmental Psychiatry for Children and Adolescents (INPD), Brazil.
- ¹⁴⁸ Melbourne Neuropsychiatry Centre, Department of Psychiatry, The University of Melbourne and Melbourne Health, Carlton South, Victoria, Australia
- ¹⁴⁹ Melbourne School of Engineering, The University of Melbourne, Parkville, Victoria, Australia
- ¹⁵⁰ Florey Institute of Neuroscience and Mental Health, Parkville, VIC, Australia
- ¹⁵¹ Department of Psychiatry, Schulich School of Medicine and Dentistry, Western University, London, ON, Canada
- ¹⁵² Department of Psychiatry, Faculty of Medicine and Centre Hospitalier Universitaire Sainte-Justine, University of Montreal, Montreal, Quebec, Canada
- ¹⁵³ Departments of Psychiatry and Psychology, University of Toronto, Toronto, ON, Canada.
- ¹⁵⁴ Departments of Physiology and Nutritional Sciences, University of Toronto, Toronto, Canada
- ¹⁵⁵ Department of Psychiatry, Faculty of Medicine, McGill University, Montreal, Qc, H3A 1Y2, Canada
- ¹⁵⁶ Douglas Mental Health University Institute, Montreal, Qc, H4H 1R3, Canada.
- ¹⁵⁷ Autism Center of Excellence, Department of Neurosciences, University of California, San Diego La Jolla, CA, USA
- ¹⁵⁸ School of Psychology, Southwest University, Chongqing 400715, P.R. China
- ¹⁵⁹ Department of Biomedical Engineering, The N.1 Institute for Health, National University of Singapore.
- ¹⁶⁰ Department of Clinical Neurosciences, University of Cambridge, Cambridge UK
- ¹⁶¹ Department of Neurology, Harvard Medical School
- ¹⁶² Department of Neurology, Boston Children's Hospital, Boston, MA 02115
- ¹⁶³ Department of Psychology, Neuroscience Institute, University of Chicago

- ¹⁶⁴ Department of Paediatrics and Wellcome-MRC Cambridge Stem Cell Institute, University of Cambridge, Hills Road, Cambridge, UK
- ¹⁶⁵ Department of Psychiatry, Universidade Federal do Rio Grande do Sul (UFRGS)
- ¹⁶⁶ National Institute of Developmental Psychiatry (INPD)
- ¹⁶⁷ Otto Hahn Group Cognitive Neurogenetics, Max Planck Institute for Human Cognitive and Brain Sciences, Leipzig, Germany
- ¹⁶⁸ Institute of Neuroscience and Medicine (INM-7: Brain and Behaviour), Research Centre Juelich, Juelich, Germany
- ¹⁶⁹ Athinoula A. Martinos Center for Biomedical Imaging, Department of Radiology, Massachusetts General Hospital, Charlestown, MA 02129, USA
- ¹⁷⁰ Centre for Population Neuroscience and Stratified Medicine (PONS), SGDP Centre, IoPPN, KCL, UK
- ¹⁷¹ PONS-Centre, Dept of Psychiatry and Psychotherapy, Campus Charite Mitte, Humboldt University, Berlin, Germany
- ¹⁷² PONS Centre, Institute for Science and Technology of Brain-inspired Intelligence (ISTBI), Fudan University, Shanghai, China
- ¹⁷³ Wallenberg Centre for Molecular and Translational Medicine, University of Gothenburg, Gothenburg, Sweden
- ¹⁷⁴ Department of Psychiatry and Neurochemistry, University of Gothenburg, Sweden
- ¹⁷⁵ Dementia Research Centre, Queen's Square Institute of Neurology, University College London, UK
- ¹⁷⁶ Center for Biomedical Image Computing and Analytics, Department of Radiology, Perelman School of Medicine, University of Pennsylvania, Philadelphia, PA, USA
- ¹⁷⁷ Departments of Neurology, Pediatrics, and Radiology, Washington University School of Medicine, St. Louis, United States
- ¹⁷⁸ SA MRC Unit on Risk & Resilience in Mental Disorders, Dept of Psychiatry and Neuroscience Institute, University of Cape Town, Cape Town, South Africa
- ¹⁷⁹ Division of Psychiatry, Centre for Clinical Brain Sciences, University of Edinburgh, UK
- ¹⁸⁰ Department of Neuroscience, Institut Pasteur, Paris, France
- ¹⁸¹ Department of Psychology, University of Cambridge, Cambridge, UK
- ¹⁸² Wu Tsai Institute, Yale University, New Haven, CT, USA
- ¹⁸³ Department of Psychiatry, University of Turku, Turku Finland
- ¹⁸⁴ Department of Clinical Medicine, University of Turku, Turku Finland
- ¹⁸⁵ Turku Collegium for Science, Medicine and Technology, University of Turku, Turku, Finland
- ¹⁸⁶ Univ. Bordeaux, Inserm, Bordeaux Population Health Research Center, U1219, CHU Bordeaux, F-33000 Bordeaux, France
- ¹⁸⁷ Department of Anesthesia, Faculty of Medicine, McGill University, Montreal, Qc, H3A 1G1, Canada
- ¹⁸⁸ Faculty of Dentistry, McGill University, Montreal, Qc, H3A 1G1, Canada
- ¹⁸⁹ Alan Edwards Centre for Research on Pain (AECRP), McGill University, Montreal, Qc, H3A 1G1, Canada
- ¹⁹⁰ University of Electronic Science and Technology of China/Cuban Center for Neuroscience
- ¹⁹¹ Institute for Neuroscience and Medicine 7, Forschungszentrum Juelich; Max Planck Institute for Human Cognitive and Brain Sciences
- ¹⁹² Department of Psychiatry & Neuropsychology, Maastricht University, Maastricht, The Netherlands
- ¹⁹³ Department of Biostatistics, Vanderbilt University, Nashville, Tennessee, USA
- ¹⁹⁴ Department of Biostatistics, Vanderbilt University Medical Center, Nashville, Tennessee, USA
- ¹⁹⁵ Division of Newborn Medicine, Fetal Neonatal Neuroimaging and Developmental Science Center, Department of Pediatrics, Boston Children's Hospital, Boston, MA 02115
- ¹⁹⁶ McConnell Brain Imaging Center, Montreal Neurological Institute, McGill University, Montreal, Quebec, Canada
- ¹⁹⁷ Clinic for Cognitive Neurology, University of Leipzig Medical Center, Leipzig, 04103, Germany
- ¹⁹⁸ The Alan Turing Institute, London NW1 2DB, UK
- ¹⁹⁹ Wellcome Centre for Human Neuroimaging, Institute of Neurology, University College London, WC1N 3AR
- ²⁰⁰ State Key Laboratory of Cognitive Neuroscience and Learning, Beijing Normal University, Beijing 100875, China
- ²⁰¹ Research Center for Lifespan Development of Brain and Mind, Institute of Psychology, Chinese Academy of Sciences, Beijing 100101, China
- ²⁰² National Basic Science Data Center, Chinese Academy of Sciences, Beijing, China
- ²⁰³ Developmental Population Neuroscience Research Lab, IDG/McGovern Institute for Brain Research, Beijing Normal University, Beijing 100875, China

²⁰⁴ Division of Clinical Geriatrics, Center for Alzheimer Research, Department of Neurobiology, Care Sciences and Society, Karolinska Institutet, Stockholm, Sweden

²⁰⁵ Faculty of Medicine, CRC 1052 'Obesity Mechanisms', University of Leipzig, Leipzig, 04103, Germany

²⁰⁶ National Basic Science Data Center, Chinese Academy of Sciences, Beijing 100190, China

²⁰⁷ Department of Electrical and Computer Engineering, National University of Singapore, Singapore

²⁰⁸ Centre for Sleep & Cognition and Centre for Translational MR Research, Yong Loo Lin School of Medicine, National University of Singapore, Singapore

²⁰⁹ N.1 Institute for Health & Institute for Digital Medicine, National University of Singapore, Singapore

²¹⁰ Integrative Sciences and Engineering Programme (ISEP), National University of Singapore, Singapore

²¹¹ Fetal Neonatal Neuroimaging and Developmental Science Center, Division of Newborn Medicine, Boston Children's Hospital, Harvard Medical School, Boston, MA 02115, USA

²¹² Melbourne Neuropsychiatry Centre, University of Melbourne, Melbourne, Australia; Department of Biomedical Engineering, University of Melbourne, Melbourne, Australia.

²¹³ SAMRC Unit on Child & Adolescent Health, University of Cape Town, South Africa

²¹⁴ Center for Translational Magnetic Resonance Research, Yong Loo Lin School of Medicine, National University of Singapore, Singapore

²¹⁵ Wellcome Trust-MRC Institute of Metabolic Science, University of Cambridge, Cambridge, CB2 0SZ

²¹⁶ Cambridgeshire and Peterborough Foundation Trust, Cambridge, CB21 5EF

²¹⁷ National Institute of Mental Health (NIMH), National Institutes of Health (NIH), Bethesda, Maryland, USA

²¹⁸ Department of Psychiatry, Escola Paulista de Medicina, São Paulo, Brazil.

* Data used in the preparation of this article was obtained from the Australian Imaging Biomarkers and Lifestyle flagship study of ageing (AIBL) funded by the Commonwealth Scientific and Industrial Research Organisation (CSIRO) which was made available at the ADNI database (www.loni.usc.edu/ADNI). The AIBL researchers contributed data but did not participate in analysis or writing of this report. AIBL researchers are listed at www.aibl.csiro.au.

** Data used in preparation of this article were obtained from the Alzheimer's Disease Neuroimaging Initiative (ADNI) database (adni.loni.usc.edu). As such, the investigators within the ADNI contributed to the design and implementation of ADNI and/or provided data but did not participate in analysis or writing of this report. A complete listing of ADNI investigators can be found at: http://adni.loni.usc.edu/wp-content/uploads/how_to_apply/ADNI_Acknowledgement_List.pdf

*** A complete listing of ARWiBo researchers can be found in the Supplementary Materials

**** The Centre for Attention Learning and Memory (CALM) research clinic is based at and supported by funding from the Medical Research Council Cognition and Brain Sciences Unit, University of Cambridge, as well as funding from the EU Horizon 2020 Personalised Medicine "LifeBrain" project (H2020-SC1-2016-2017, Topic SC1-PM-04-2016). The lead investigators are Duncan Astle, Kate Baker, Susan E. Gathercole, Joni Holmes, Rogier A. Kievit, and Tom Manly. Data collection was assisted by a team of researchers and PhD students that includes Danyla Akarca, Joe Bathelt, Giacomo Bignardi, Sarah Bishop, Erica Botanic, Lara Bridge, Diandra Bkric, Annie Bryant, Sally Butterfield, Elizabeth Byrne, Gemma Crickmore, Edwin Dalmaijer, Fánchea Daly, Tina Emery, Grace Franckel, Laura Forde, Delia Fuhrmann, Andrew Gadie, Sara Gharooni, Jacalyn Guy, Erin Hawkins, Agnieszka Jaroslawska, Sara Joeghan, Amy Johnson, Jonathan Jones, Elise Ng-Cordell, Sinéad O'Brien, Cliodhna O'Leary, Joseph Rennie, Ivan Simpson-Kent, Roma Siugzdaite, Tess Smith, Stepheni Uh, Francesca Woolgar, Mengya Zhang, and Natalia Zdorovtsova. We thank the many professionals working in children's services in the southeast and east of England for their support and to the children and their families for giving up their time to visit the clinic, and the radiographer for facilitating pediatric scanning.

***** The Cambridge Centre for Ageing and Neuroscience (Cam-CAN) research was supported by the Biotechnology and Biological Sciences Research Council (BB/H008217/1), as well as funding from the Medical Research Council Cognition and Brain Sciences Unit, and the EU Horizon 2020 Personalised Medicine "LifeBrain" project (H2020-SC1-2016-2017, Topic SC1-PM-04-2016). We thank the Cam-CAN respondents and their primary care teams in Cambridge for their participation in this study. Further information about the Cam-CAN corporate authorship membership can be found at <http://www.cam-can.org/index.php?content=corpauth#12>.

***** Data used in this article were obtained from the developmental component 'Growing Up in China' and the standardization component '3R-BRAIN' of Chinese Color Nest Project (<https://github.com/zuoxinian/CCNP>). More information of the CCNP team can be found at the DeepNeuro Lab (<http://deepneuro.bnu.edu.cn/?p=163>).

***** Data was downloaded from the COllaborative Informatics and Neuroimaging Suite Data Exchange tool (COINS; <http://coins.mrn.org/dx>) and data collection was performed at the Mind Research Network, and funded by a Center of Biomedical Research Excellence (COBRE) grant 5P20RR021938/P20GM103472 from the NIH to Dr. Vince Calhoun.

***** The ENIGMA Developmental Brain Age working group principally consists of Drs. James Cole, Niall Bourke, Heather Whalley, David Glahn, Laura Han, Francesca Biondo, Katherine Karlsgodt, Carrie Bearden, Jakob Seidlitz, Richard Bethlehem, Eileen Xu, Marieke Bos, Sam Mathia, Sophia Frangou, Miruna Carmen Barbu, Yoonho Chung, and Aaron Alexander-Bloch

***** Data used in the preparation of this article were obtained from the Harvard Aging Brain Study (HABS - P01AG036694; <https://habs.mgh.harvard.edu>). The HABS study was launched in 2010, funded by the National Institute on Aging, and is led by principal investigators Reisa A. Sperling MD and Keith A. Johnson MD at Massachusetts General Hospital/Harvard Medical School in Boston, MA.

***** Data used in this article were obtained from the Korean Longitudinal Study on Cognitive Aging and Dementia (KLOSCAD) (<https://recode.re.kr>).

***** A full list of NSPN consortium members can be found at: <https://www.nspn.org.uk/nspn-team/>

***** The POND network is a Canadian translational network in neurodevelopmental disorders, primarily funded by the Ontario Brain Institute.